

# Fuzzy Neural Network for Studying Coupling between Drilling Parameters

Li Yang,\* Tianyi Liu, Weijian Ren, and Wenfeng Sun

Cite This: *ACS Omega* 2021, 6, 24351–24361

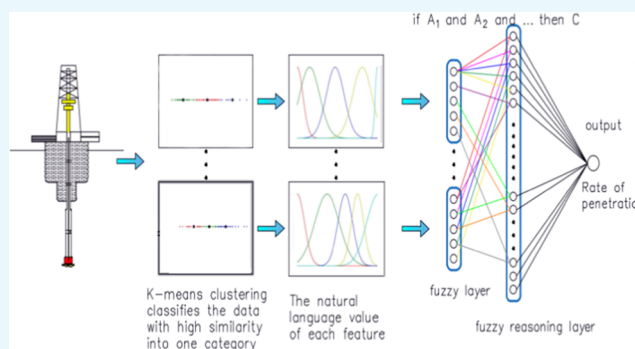
Read Online

ACCESS |

Metrics &amp; More

Article Recommendations

**ABSTRACT:** The rate of penetration (ROP) is an index used to measure drilling efficiency. However, it is restricted by many factors, and there is a coupling relationship among them. In this study, the random forest algorithm is used to sort influencing factors in order of feature importance. In this way, less influential factors can be removed. A fuzzy neural network (FNN) is applied to the field of drilling engineering for the first time, aiming at the coupling problem to predict the ROP. Fuzzification is an important part of training and realizing FNN, but research on this topic is currently lacking. In this study, K-means are used to divide the data with high similarity into a fuzzy set, which is used as the initialization parameter for the second layer of the FNN. The data of Shunbei No. 1 and 5 fault zones in Xinjiang are collected and trained. The results show that the mean value of the coefficient of determination  $R^2$  is 0.9668 under 10 experiments, which is higher than those obtained from a back propagation neural network and multilayer perceptron particle swarm optimization methods. Therefore, the effectiveness and feasibility of the model are verified. The proposed model can improve drilling efficiency and save drilling costs.



## 1. INTRODUCTION

The development of oil and gas is inseparable from the advancements in drilling technology. With the increasing demand for energy exploitation, the development of drilling also needs further technical improvement. However, drilling engineering is becoming increasingly complex. The main challenge is to achieve a high drilling speed and low cost.<sup>1</sup> Therefore, improving drilling technology is an important means and measure to address the aforementioned problem.

The rate of penetration (ROP), which is the drilling distance of the bit in unit time, is an index used to evaluate drilling efficiency. Drilling efficiency can be improved using a proper combination of drilling parameters.<sup>2</sup> However, because of uncertainty factors in the drilling process, establishing a general model in drilling engineering is problematic. A complicated coupling relationship exists in each link.<sup>3</sup> Consequently, the predicted results of the model are different from the actual drilling speed. At present, research methods have been developed from single-parameter research to multiobjective and multiparameter optimization. The global research on drilling speed prediction has changed from mathematical models to artificial intelligence algorithms.<sup>4</sup> As a representative of traditional machine learning, support vector regression (SVR)<sup>5,6</sup> has a better fitting effect in experimental than other machine-learning methods [such as K-nearest neighbors (KNN), linear regression (LR), polynomial regression, and

decision tree], considering the drilling characteristics of highly nonlinear, complexity, and multivariate in the drilling process. However, SVR is difficult to implement when processing large data samples as a quadratic programming problem is solved. This process takes a significant amount of computation time. Further, gradient boosting decision tree,<sup>7</sup> random forest,<sup>8</sup> and other ensemble learning studies are useful for drilling rate prediction. With the progress in research, the three-layer back propagation (BP) neural network is the current mainstream machine-learning algorithm used for predicting the drilling speed.<sup>9–12</sup> A regression model of influencing factors and the drilling speed was established. However, its degree of fitting requires improvement and optimization.<sup>13,14</sup> Shi et al.<sup>15</sup> proposed the extreme learning machine (ELM) and upper-layer solution aware (USA) methods to predict the drilling rate, where the prediction accuracy was higher than that of a BP neural network. Ashrafi et al.<sup>16</sup> found the best ROP value in terms of the shortening drilling time and reducing the drilling

Received: April 21, 2021

Published: September 15, 2021

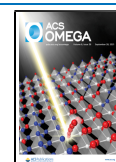


Table 1. Partial Data Set Samples

diameter no.		1	2	3	4	5	6
drill diameter		311.2	310.2	250.8	165.1	444.5	149.2
drilling time		108.4	125.5	167.5	121.2	105.4	25.2
depreciation rate per meter		0.0006	0.0011	0.0011	0.0025	0.0006	0.0130
ROP		3.45	1.79	1.60	2.58	14.11	0.91
drilling parameter	WOB	260	280	280	200	80	200
	speed	57	60	65	88	60	60
	displacement	50	50	48	55	60	40
	riser pressure	20	20	20	15	18	16
properties of drilling fluid	density	1.22	1.22	1.24	1.17	1.17	1.25
	funnel viscosity	49	49	58	47	56	48
	sediment concentration	0.2	0.2	0.2	0.2	0.2	0.2
	API filter vector	4	3.6	3.4	5	6	3.4
bit hydraulic parameter	bit pressure drop	2.2	2.22	2.06	5.14	1.87	1.44
	annular pressure loss	17.8	1.78	17.94	9.86	16.13	14.56
	jet impact force	3456.7	3485.0	3237.9	5692.68	3748.42	2266.7
	jet speed	56.67	56.67	54.4	88.46	53.4	45.33
	bit water power	110.05	110.95	98.96	282.92	112.44	57.73
	bit specific water power	1.45	1.46	1.3	3.72	1.48	1.26
	minimum return speed of the drill pipe	0.82	0.82	0.79	0.91	0.99	1.32
	minimum return speed on the drill string	1.64	1.64	1.58	1.81	1.97	1.91
	pump power utilization	11	11.09	10.31	34.29	10.41	9.02

cost. Owing to the error of multiple regression, the genetic algorithm (GA), particle swarm optimization (PSO), biogeography-based optimizer, and imperialist competitive algorithm (ICA) were used to develop and train eight hybrid neural artificial neural networks, and they were compared. Particle swarm optimization multilayer perceptron and PSO-radial basis function proved that the neural network has higher efficiency and reliability in drilling rate prediction. Sabah et al.<sup>17</sup> evaluated the applicability of such a model for actual engineering applications. A comparative experiment was conducted to identify which machine-learning method provided the most accurate and reliable ROP prediction; the multilayer perceptron particle swarm optimization (MLP-PSO) model showed excellent performance in all comparative experiments. Liao et al.<sup>18,19</sup> studied and analyzed the influence of rock strength on the mechanical drilling speed. Therein, the parameters of thrust, speed, flushing medium, and compressive strength were analyzed using the artificial colony algorithm. The rock strength was classified into three grades to improve the performance of the mechanical drilling speed and to determine the best parameters of the three levels. There are many factors that affect ROP, which leads to increased complexity of the model and an increase in the calculation amount. Thus, dimensionality reduction is necessary as part of data preprocessing. Eskandarian<sup>8</sup> used the fscaret package in an R environment to calculate the importance and ranking of input parameters. According to the results of feature ranking, weight on bit (WOB) and mud weight (MW) had the greatest influence on the ROP. The experiment proved that the root-mean-squared error could be reduced by appropriately extracting important features, and the prediction accuracy of the model had been improved to a certain extent. Anand<sup>20</sup> determined that the diameter of drill bit was the largest influencing factor, followed by the feed rate and the spindle speed, through gray relational grade analysis. Hassan et al.<sup>21</sup> improved the real-time drilling operation using the ratio of permeability to mechanical specific energy to evaluate the feasibility and limitations of several models in practical applications.

At present, the focus of optimization algorithm research is on drilling efficiency improvement, ignoring the influence of complex working conditions on control decision-making and stability control. Due to the lack of drilling knowledge in general models, technology and practical engineering cannot be deeply integrated. To satisfy the dialectical relationship of mutual connection and mutual restriction among various parameters, a fuzzy control model was proposed, and its core fuzzy rule table expresses this objective law. Owing to the complementarity of fuzzy control and neural networks, a fuzzy neural network (FNN) was applied in various fields of research.<sup>22–25</sup>

In this study, an FNN is applied to the forecast of drilling ROP, and complex problems are solved by human thinking. Artificial intelligence is used to identify possible correlations among the parameters. The basic regression model is constructed by combining fuzzy control with a neural network. On this basis, this study uses the random forest algorithm to extract feature importance and remove the least-important factors to balance the model complexity and the fitting effect and allow the model architecture to be simplified. Finally, The FNN model is optimized, and the features of the same dimension are divided into fuzzy sets by a clustering algorithm; in the process of fuzzification, the interval range of fuzzy sets is standardized to increase the interpretability of linguistic values.

## II. FEATURE SELECTION

Feature selection has always been a major problem in feature engineering. Its purpose is to find the optimal feature subset. Feature selection removes irrelevant and redundant data and eliminates less relevant factors, which reduce the calculation time. This improves the learning accuracy and promotes better understanding of the learning model or data.<sup>26–28</sup> Some unimportant factors do not only increase the complexity of modeling but also reduce the accuracy of prediction. Therefore, the feature importance of influencing factors should be analyzed and unimportant factors should be removed. To better retain the physical meaning of the parameters, random forest is introduced to perform importance ranking.

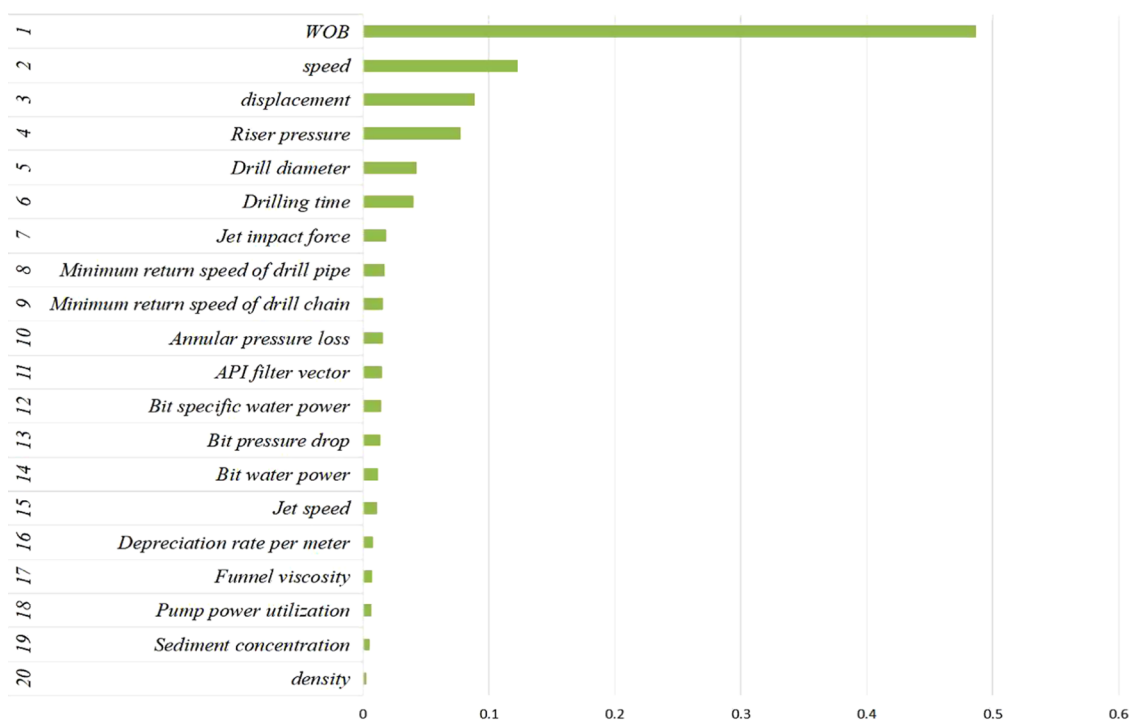


Figure 1. Feature importance ranking.

**II.I. Random Forest Algorithm.** Random forest is an integrated learning algorithm.<sup>29,30</sup> It has good tolerance for outliers and strong robustness. Its principle is to extract parts of the samples repeatedly from the sample set to generate multiple decision trees. The feature importance is evaluated using data out of bag (OOB). The verification error of the  $j$ th decision tree is calculated as  $E_j$  using data outside the bag. The first characteristic of the data outside the bag under evaluation is randomly disrupted, and the verification error  $E'_{ij}$  of the  $j$ th decision tree is calculated again. Subsequently, the sum of the squares of the differences of these two verification errors is computed using the following equation

$$f_i = \sum_j^n (E'_{ij} - E_j)^2 \quad (1)$$

where  $n$  is the number of decision trees. The value of  $n$  can be used as a reference value of the importance of a single feature; that is, the larger the value, the greater the impact of the disturbing feature, and the more important the feature.

Table 1 shows a partial sample set of 21 dimensional data, which includes fixed parameters (drill diameter, drilling time, depreciation rate per meter), drilling parameters (WOB, speed, displacement, riser pressure), drilling fluid performance (density, funnel viscosity, sediment concentration, API filter vector), and bit hydraulic parameters (bit pressure drop, annular pressure loss, jet impact force, etc.).

The drilling data of the Shunbei oilfield provide comprehensive and referential influencing factors. According to the results shown in Figure 1, there are 20 groups of characteristics in the data. The most important factor is WOB, the degree of importance of which reaches 0.487. Other relatively large factors are the rotational speed, displacement, riser pressure, bit diameter, and pure drilling time. These six characteristics are used as an input. The importance of the six parameters is shown in Table 2.

Table 2. Feature Importance

no.	features	importance degree
1	WOB	0.486897
2	speed	0.122810
3	displacement	0.088386
4	riser pressure	0.077281
5	drill diameter	0.042577
6	drilling time	0.039879

### III. METHODOLOGY

**III.I. General Description of Fuzzy Control.** There are essential differences between the human brain and a computer. The human brain can handle and judge fuzzy phenomena.<sup>31,32</sup> Fuzziness generally exists in human thinking and language communication, which is a manifestation of uncertainty. When human beings describe natural phenomena, they have a fuzzy concept in their brain. After learning and understanding an experience, they make a fuzzy division of the general objective law and make a better decision; this process is defined as “fuzzification”. Usually, an expert system is based on expert experience. Fuzzy control is based on human thinking, taking an appropriate strategy to control a complex process.

**III.II. Basic Principle of the Fuzzy Neural Network.** Each layer of the FNN corresponds to the steps of the Mamdani-type fuzzy control system,<sup>33</sup> as shown in Figure 2.

The first layer is the input layer, and each component of the input vector corresponds to each node of the first layer, which transmits the input value  $x = [x_1, x_2, \dots, x_n]$  to the next layer.

The second layer is the fuzzification layer, where each input corresponds to its own membership function. Each membership function represents the value of language variables. The membership function is represented by a Gaussian function

$$\mu_i^j = e^{-(x_i - c_{ij})^2 / \sigma_{ij}^2} \quad (2)$$

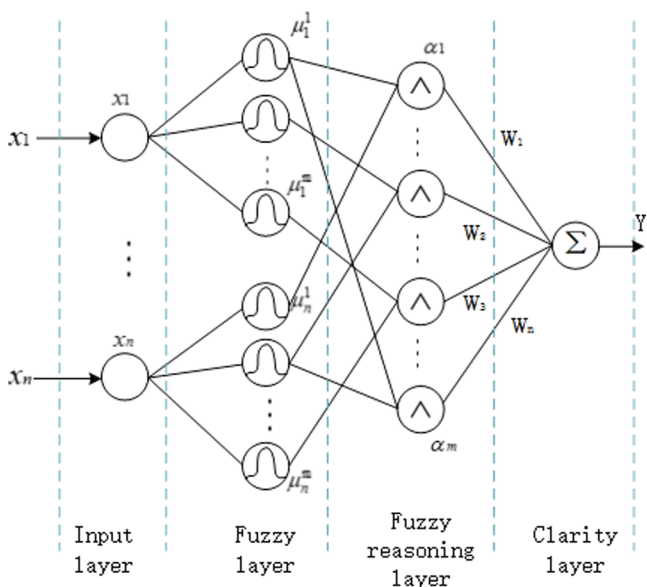


Figure 2. Fuzzy network model.

Each node in the third layer represents a fuzzy rule, which is used to match the antecedents of the fuzzy rule and to calculate the applicability of the rule

$$\alpha_i = \min\{\mu_1^{i_1}, \mu_2^{i_2}, L, \mu_n^{i_n}\} \tag{3}$$

The fourth layer is the clarity layer, which converts the fuzzy value into the clarity value and outputs it

$$y = \sum_{i=1}^m \omega_i \alpha_i \tag{4}$$

**III.III. K-Means Algorithm.** The FNN is trained using three parameters: the center value, the width of the membership function, and the weight of the last layer. To obtain better results, the input is processed, and the traditional method of random initialization or equidistant division of the membership function is improved. The data with high similarity are divided into classes by clustering, which better represents the initial language value variables so that the model can achieve a better training effect. This partition is also called hard clustering.<sup>34</sup> The data set is divided into k parts by K-means clustering, and K clustering points are found as the central values of the membership function. These central values are introduced into the network as the parameters of the initialization membership function.

Given the sample set  $D = \{x_1, x_2, \dots, x_m\}$ , the k-means algorithm minimizes the square error of clustering

$$E = \sum_{i=1}^k \sum_{x \in C_i} \|x - \mu_i\|^2 \tag{5}$$

$\mu_i = \frac{1}{|C_i|} \sum_{x \in C_i} x$  is the mean vector of cluster  $C_i$ . The smaller the E value, the higher the similarity of samples in the cluster.

The data of each dimension are clustered, and each dimension adopts five membership functions. The center values of the first and last membership functions are the upper and lower bounds of the value, respectively. The K-means clustering results are shown in Figure 3.

The initial value of the membership function width is as follows

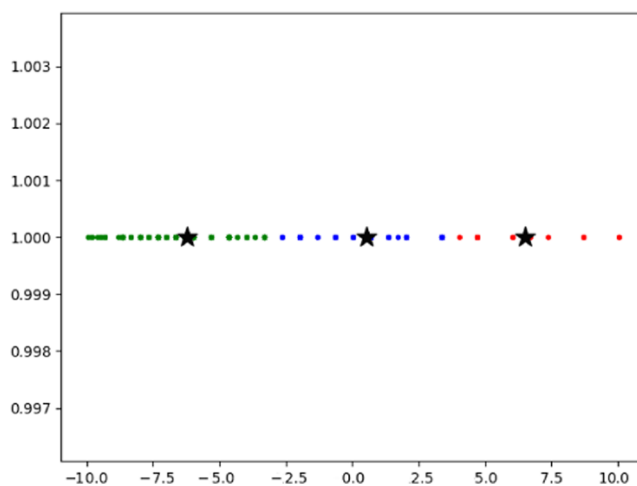


Figure 3. K-means clustering results.

$$\sigma_i = \frac{1}{2}(c_i + 1 - c_i) \quad (0 < i < k - 1) \tag{6}$$

The membership function of the neural network training is initialized after clustering, and the result is shown in Figure 4,

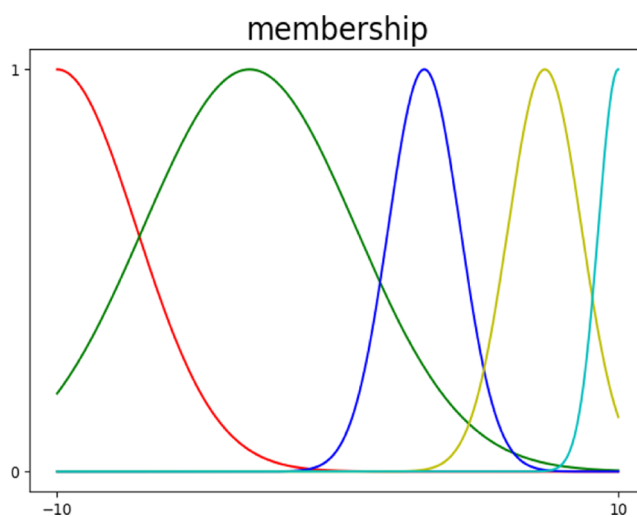


Figure 4. Initial membership.

where all of the information is retained. During the training, the neural network parameters should only be adjusted slightly to obtain satisfactory results. Figure 5 shows the effect of randomly initializing the center value and the width of the Gaussian function. It can be observed that a lot of information will be lost after random initialization, which may seriously affect the model accuracy.

**III.IV. Model Training.** The loss function is used to measure the degree of the prediction error. Because the number of training sets is limited, we choose the square loss function, which is convenient to calculate

$$E = \frac{1}{2}(Y - F(X))^2 \tag{7}$$

where Y and F(X) represent the desired output and the actual output, respectively.

Because the square error loss enlarges the distance between the predicted value and the real value in the calculation, the

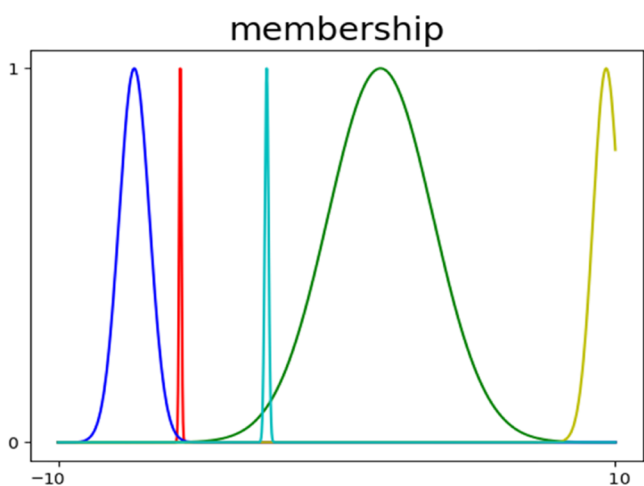


Figure 5. Random initialization membership.

output with a larger error is given greater punishment, which is conducive to the calculation of the error gradient. The parameters are updated by error BP

$$\omega_i(k+1) = \omega_i(k) - \beta \frac{\partial E}{\partial \omega_i} \quad (i = 1, 2, \dots, r) \quad (8)$$

$$C_{ij}(k+1) = C_{ij}(k) - \beta \frac{\partial E}{\partial C_{ij}} \quad (i = 1, 2, \dots, m; j = 1, 2, \dots, n) \quad (9)$$

$$\sigma_{ij}(k+1) = \sigma_{ij}(k) - \beta \frac{\partial E}{\partial \sigma_{ij}} \quad (i = 1, 2, \dots, m; j = 1, 2, \dots, n) \quad (10)$$

where  $\omega$  represents the last layer weight of the network, and its physical significance is that  $\omega_i$  is equivalent to the central value of the output Y membership function,  $C_{ij}$  and  $\sigma_{ij}$  represent the center and the width of the membership function, and  $\beta$  represents the learning rate.

**III.V. Training Process Improvement.** In the process of training the membership function, the center value and the width of the membership function will constantly increase or decrease. This is because the direction of the gradient descent does not change during training. Therefore, the network should be improved by adding a limited interval in each Gaussian membership function, and the central values of the five membership functions are  $[-11, -9]$ ,  $[-7, -3]$ ,  $[-2, 2]$ ,  $[3, 7]$ , and  $[9, 11]$ , respectively.

Table 3. Partial Sample Set

no.	WOB (kn)	speed (rpm)	displacement (L/s)	pressure (MPa)	time (h)	diameter (mm)	ROP (m/h)
1	80	60	30	18	105.67	311.2	14.08
2	280	65	37.2	11.5	113.66	310.2	1.92
3	100	70	35	15	107	250.88	5.04
4	80	50	30	21	102.5	215.9	6.38
5	80	40	40	20	195	250.88	6.54
6	120	70	33	19	45	250.88	2.97
7	40	50	55	20	45	311.2	21.07
8	60	42	30	18	217	250.88	5.79

$$\begin{cases} C^{\text{new}} = C^{\text{new}}, & \text{if}(L < C^{\text{new}} < H) \\ C^{\text{new}} = C^{\text{old}}, & \text{otherwise} \end{cases} \quad (11)$$

where  $L$  and  $H$  are the upper and lower limits of the corresponding limited interval.

The width of the membership function is limited to  $[1, 4]$ .

$$\begin{cases} \sigma^{\text{new}} = \sigma^{\text{new}}, & \text{if}(L < C^{\text{new}} < H) \\ \sigma^{\text{new}} = \sigma^{\text{old}}, & \text{otherwise} \end{cases} \quad (12)$$

The normalized membership function will retain the information of each language value to the maximum extent and will not cause information loss owing to improper training. When the training exceeds this limited interval, the last value will be retained to ensure that the model can clearly express the meaning of each fuzzy language (FL) value.

#### IV. CASE ANALYSIS

When the Shunbei oilfield was discovered, it became an important area of resource strategy alternation in the west of

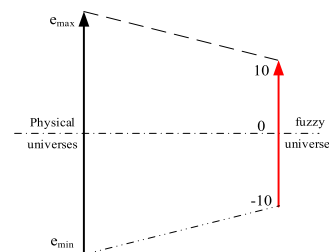


Figure 6. Fuzzification process.

Sinopec. Affected by the fault movement, the bottom hole temperature of the northwest oilfield is high, and the controllable parameters are constantly changing in the process of drilling.<sup>35</sup> To find the optimal combination of parameters, according to the previous random forest feature extraction importance results, six relatively important performance indexes are selected: WOB, speed, displacement, riser pressure, drilling time, and bit diameter as the inputs, and ROP as the output. The data are fitted by training the parameters of the membership function and the weight of the last layer. The number of membership degrees is set to follow the rationality; too much or too little will have a certain impact on the model. If the number of the fuzzy language value is less, the sensitivity to the data will be reduced. However, large size data will lead to high complexity of the model. Specifically, when the input quantity is large, the number of fuzzy rules will increase exponentially. The number of fuzzy language values is five to balance the influence of the two

Table 4.  $R^2$  of 10 Experiments of the FNN Model under the Action of Different Optimizers

no.	1	2	3	4	5	6	7	8	9	10	
$R^2$	Adam optimizer	0.9706	0.9718	0.9411	0.9701	0.9705	0.9618	0.9714	0.9705	0.9684	0.9715
	SGDM optimizer	0.9639	0.9724	0.9408	0.9667	0.9711	0.9701	0.9712	0.9679	0.9614	0.9698

Table 5. Average  $R^2$  of FNN in 10 Experiments at Different Learning Rates under the Action of Different Optimizers

learning rate	0.1	0.2	0.4	0.6	
$R^2$	Adam	0.9602	0.9668	0.9598	0.9644
	SGDM	0.9605	0.9655	0.9523	0.9502

aspects in which each input is divided into five parts. Five linguistic variables are represented by five Gaussian membership functions, which are represented by “lowest”, “low”, “medium”, “high”, and “highest”. Therefore, the basic model of the FNN is constructed.

**IV.I. Data Preprocessing.** The data of Shunbei No. 1 and 5 fault zones in Shaya County, Xinjiang, are used as training samples. A total of 1100 sets of data from 45 strata including Triassic Halahatang formation, Permian aqia group, Carboniferous Kalashayi formation, and Carboniferous Bachu formation are used as samples. Six parameters that have a great influence on ROP are selected as a training sample set to verify the established parameter optimization model using the FNN, thus, determining the feasibility of the method. Table 3 shows some sample data.

The acquired samples need to be processed to convert the actual continuous field into a finite integer discrete field and to adjust the variables so as to match the adjacent modules well. Figure 6 shows the process of mapping the object theory domain to the fuzzy theory domain.

The physical and fuzzy universes are set to  $X = [e_{\min}, e_{\max}]$  and  $Y = [-10, 10]$ , respectively. Hence, the general formula of continuous universe is expressed as follows

$$y = \frac{20}{e_{\max} - e_{\min}} \left( x_0 - \frac{e_{\max} + e_{\min}}{2} \right) \quad (13)$$

where  $e_{\max}$  and  $e_{\min}$ , respectively, correspond to the maximum and minimum values of each feature subset. The quantitative factors of mapping the physical universe to the fuzzy universe are as follows

$$y = \frac{20}{e_{\max} - e_{\min}} \quad (14)$$

**IV.II. Cross Validation.** To ensure that the model does not generate random errors owing to the random allocation of training and test sets from the original data, we performed 10-fold cross validation. The data set was evenly divided into 10 parts, 9 of which were considered as the training set and the remaining 1 as the test set for an experiment. Thereafter, one copy from the training set was taken in turn as the new test set and the original test set was put into the training set. This was performed in turn in 10 sets. The model with the smallest absolute mean error was considered as the final model, whereas the average of the absolute mean error of the results of 10 experiments was used to evaluate the model.

The model was built using Python language in the Anaconda development environment. In the experiment, the data were

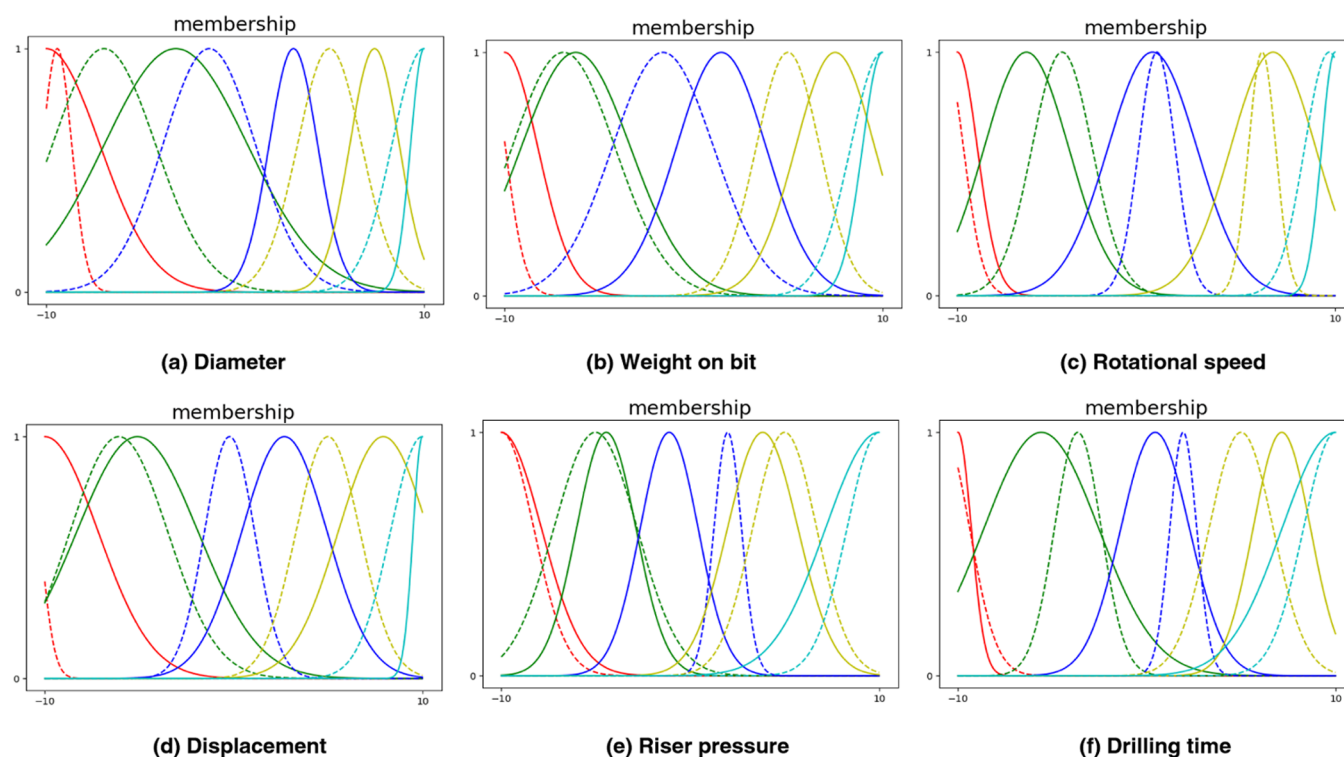


Figure 7. Changes in the membership function of input (a–f) language value variables.

Table 6. Several Fuzzy Rules Obtained by FNN

no.	input variable											
	diameter			WOB			rotational speed			displacement		
	input	FL	membership	input	FL	membership	input	FL	membership	input	FL	membership
1	215.9	high	0.9092	60	low	0.7234	60	low	0.7214	25	lowest	0.7168
2	215.9	high	0.9092	60	low	0.7234	60	low	0.7214	25	lowest	0.7168
3	311.2	highest	0.6844	80	medium	0.8635	40	lowest	0.9786	32	medium	0.9985
4	149.2	low	0.3432	35	lowest	0.9204	25	lowest	0.5385	14	lowest	0.5248
5	149.2	low	0.3433	40	lowest	0.6844	25	lowest	0.5385	12	lowest	0.4843

no.	input variable						output variable		
	drilling time			riser pressure			ROP		
	input	FL	membership	input	FL	membership	output	FL	membership
1	85	high	0.7970	20	high	0.9873	4.5022	lowest	0.8438
2	247	highest	0.8394	30	highest	0.2940	12.876	low	0.7168
3	153	medium	0.6874	20	high	0.9873	25.926	medium	0.9004
4	82.5	low	0.6413	20	high	0.9873	2.9886	lowest	0.5057
5	50	lowest	0.7864	20	high	0.9873	2.9060	lowest	0.5162

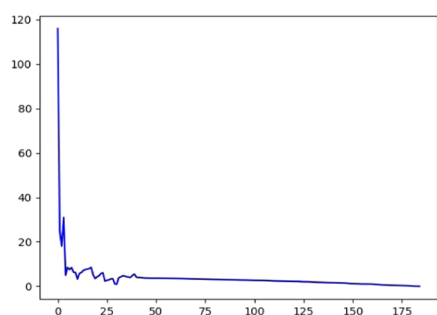


Figure 8. Train error of the FNN.

divided by the model\_selection module in the sklearn library. Then, 10 experiments were conducted to evaluate the generalization ability of the FNN on the data set independence of the training data through cross validation. The mini batch gradient method was used for the training model. The initial learning rate was set to 0.2. Under the action of different optimizers, the network parameters affecting model training and model output were updated and calculated to approximate or attain the optimal value. The determination coefficient  $R^2$  was

used as the evaluation standard of the model. Table 4 shows the  $R^2$  values of 10 experiments. Table 5 shows the average  $R^2$  of 10 experiments of FNN at different learning rates.

The experimental results demonstrate that most of the accuracy of the Adam optimizer is slightly higher than that of the SGDM optimizer. Therefore, the updated model of the Adam optimizer is selected in this experiment.

**IV.III. Results and Discussion.** The membership changes of the input language value variables are shown in Figure 7. The dotted line represents the membership function after iterations, and the solid line is the initial membership function, which can clearly express the changes in each membership function. After training, the membership function width of ROP, displacement, riser pressure, and drilling time becomes narrower, and the adjacent intersection area is smaller, indicating that the sensitivity is higher. The membership function of the diameter also becomes narrower, but the distribution is relatively uniform. The membership function of WOB is relatively wide, and there is no clear change in the width after the update, indicating that it has a strong adaptability to parameter changes and good robustness. However, the central value of membership changes greatly, and the semantic value changes noticeably.

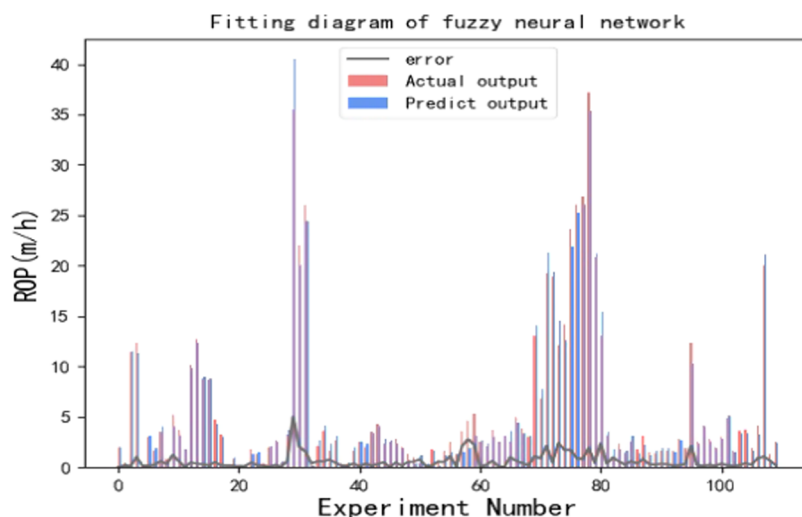


Figure 9. Predicted value and the actual output of FNN.

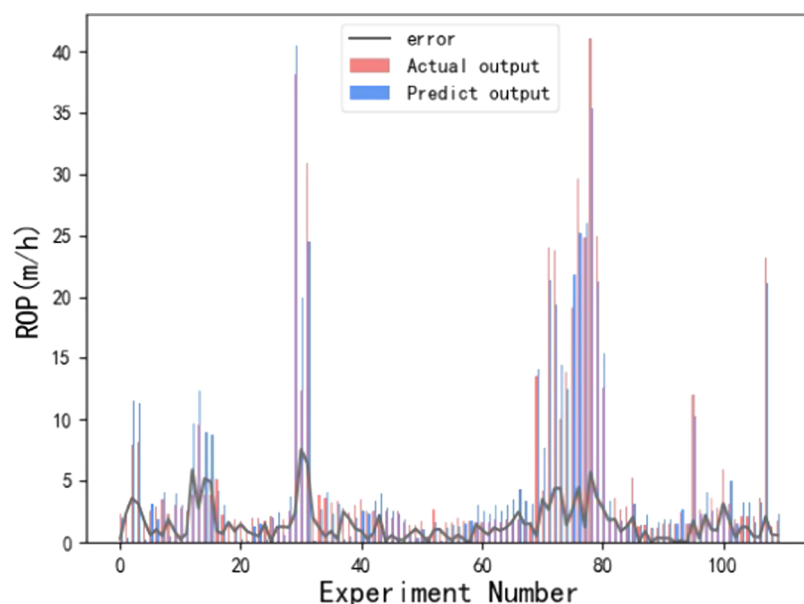


Figure 10. Predicted value and the actual output of SVR.

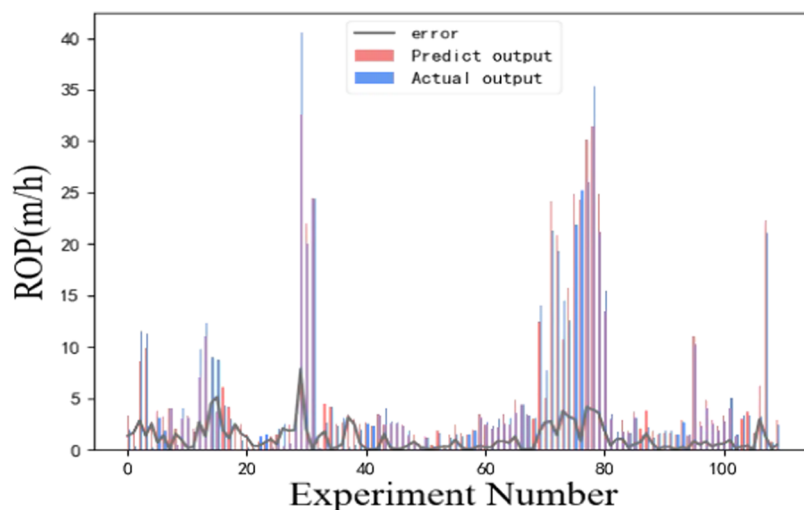


Figure 11. Predicted value and the actual output of BPNN.

The Shunbei 5–5 h well, with a drilling depth of 8520 m, is an ultradeep well drilled in the Shunbei oilfield, which has set the deepest drilling record in Asia.<sup>36</sup> The fuzzy language (FL) value of some stratum data in the region was selected to extract the fuzzy rules from the model. Several extracted fuzzy rules are listed in Table 6.

To verify whether the extracted fuzzy rule table is correct considering the fitting effect of the model, the FNN training set error and the test set fitting effect are shown in Figures 8 and 9.

Figure 8 shows the initial decline curve of the training result of the FNN. The standard training error was set to  $10^{-3}$ . The fluctuation is large in the early stage of decline because of the membership function update. When the error is large, the range of the change of the membership function increases. Therefore, the language value variable corresponding to each element is modified. When the error is small, the membership function is determined. The fitting effect of the test set is shown in Figure 9, where output 1 is the output result of the model, output 2 is the actual output result of the test set, and error is the absolute value of the difference between the actual output and the model

output. The absolute value of the average error is 0.5090. The model has a good fitting effect for different wells in the same block. Thus, the fuzzy rules extracted from Table 2 are confirmed to be applicable.

To verify the superiority of the FNN, the simulation results of the FNN were compared to those of traditional SVR,<sup>6</sup> BPNN,<sup>9</sup> and MLP-PSO<sup>17</sup> models. The Gaussian kernel function is used for SVR, penalty parameter  $C$  is set to 1.25, slack variable  $\epsilon$  is set to 0.05, and the stop condition set to the training error is less than  $10^{-3}$ . The number of layers of the BP neural network is set to three layers, the number of neurons in the input layer is six, and the number of neurons in the output layer is one. The sigmoid function is used as the activation function. MLP-PSO overcomes the disadvantages that can occur with the gradient descent in the training method, such as slow learning rates and trapping at local minima, and uses PSO to update the weights and offsets between neurons. In this experiment, the following PSO parameters were used: population size of 80; individual learning factor  $C1$  and social learning factor  $C2$  of 0.7; inertial weight of 0.9; and standard training error of  $10^{-3}$ . In addition,



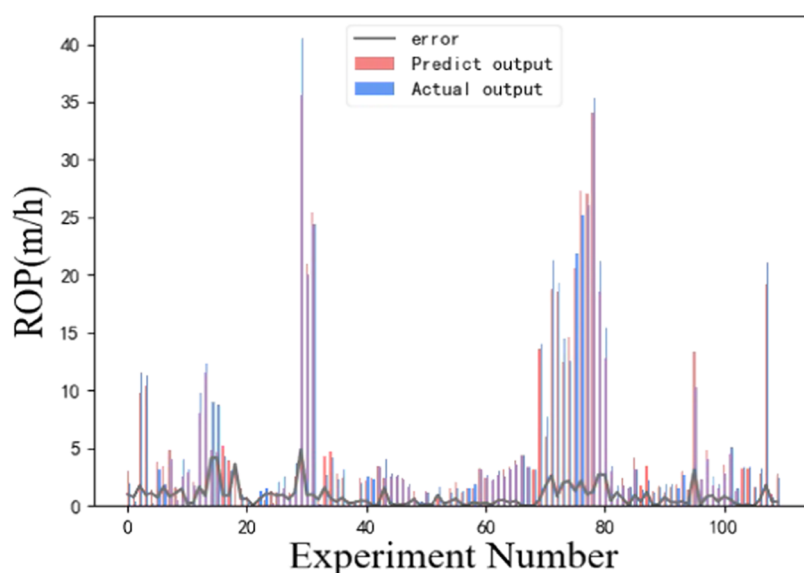


Figure 12. Predicted value and the actual output of MLP-PSO.

Table 7. Determination Coefficient Values of BP Neural Network Fitting under Different Parameter Settings

$R^2$	learning rate		
number of neurons	0.1	0.2	0.4
10	0.7403	0.7386	0.7273
12	0.8128	0.8315	0.9197
15	0.6901	0.8128	0.7401

the search range of space is adjusted, and the training error is used as the fitness function. The BPNN and MLP-PSO models are used to train and test the sample data after normalization. Figures 10–12 compare the predicted and actual values of three methods, respectively.

Table 7 shows the average  $R^2$  values from 10 experiments of BPNN fitting for 9 different parameter settings. The number of neurons in the hidden layer is set to 10, 12, and 15, and then the  $R^2$  values with learning rates of 0.1, 0.2, and 0.4 are calculated.

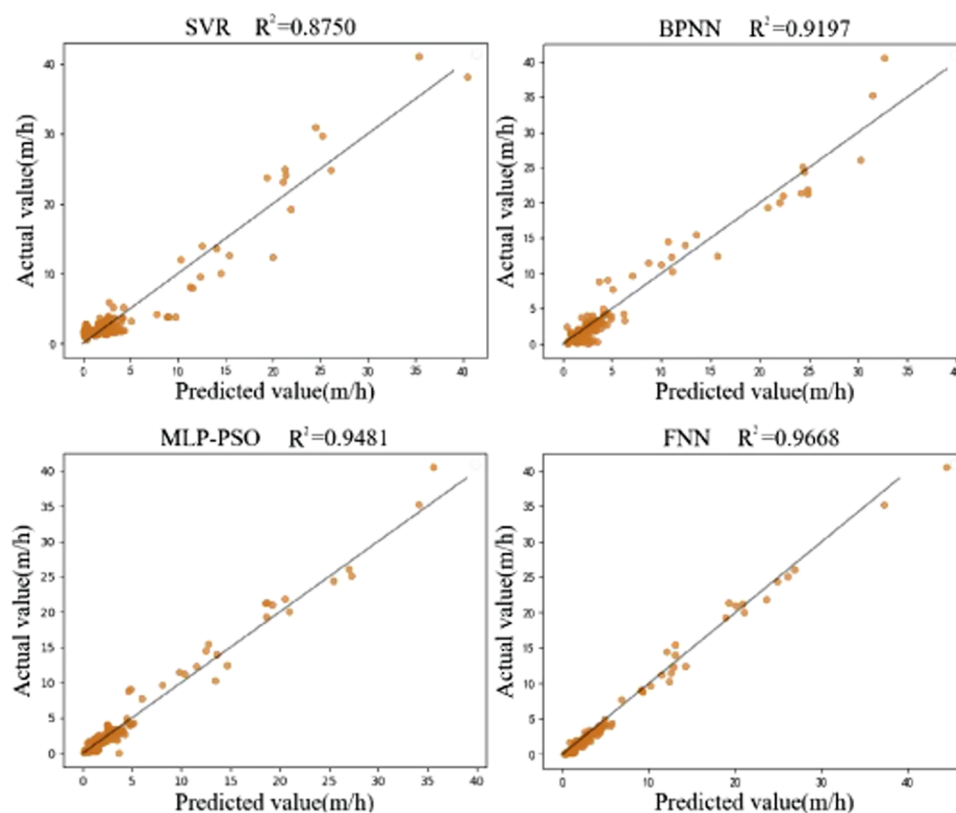
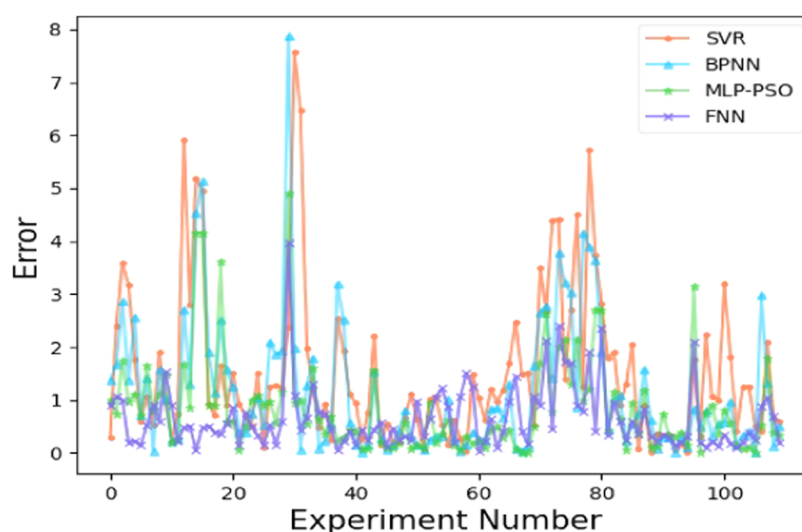


Figure 13. Relationship between predicted and actual values.



**Figure 14.** Comparison of the prediction errors.

Figure 13 shows the relationship between the actual value and the predicted value from the four different models. The abscissa represents the predicted value, the ordinate represents the actual value, and the diagonal line represents the approximation degree between the predicted and actual values. The closer the line is to the data set, the better the fitting effect, corresponding to higher prediction accuracy. The average  $R^2$  of 10 experiments using the four methods is calculated. Figure 14 compares the prediction error of the four methods. In terms of the fitting effect, FNN is better than other methods, which proves the superiority of the model.

## V. CONCLUSIONS

In this paper, the coupling relationship between the parameters in the process of drilling is considered, and an FNN model is established. Six parameters, such as WOB and rotational speed, are optimized using data from Shunbei No. 1 and 5 fault zones in Shaya County, Xinjiang. By matching the credibility of the total premise of each rule, the total output of each rule is obtained by performing small operations. Based on the obtained experimental results, the contributions of this study are as follows:

1. The random forest algorithm was used to calculate the importance of features. As a result, six features with greater importance were obtained, which reduced the complexity of the model. In the process of the fuzzy layer of FNN, K-means was used to initialize the central value of the membership degree, and the FNN model was optimized.
2. Using big data processing to express data relevance in the form of experience could effectively solve the changes in the output values of various parameters in different ranges. Therefore, the proposed algorithm is more reflective of human thinking than traditional algorithms.
3. According to the training error of the training set and the fitting effect of the test set, the performance of the improved fuzzy neural network model is better than that of the traditional BP neural network, MLP-PSO, and SVR model.
4. The simulation results show that the proposed method has a good prediction effect on ROP in the construction process of the area, and the model can provide technical

reference for drilling automation in the Shunbei oil and gas field.

In this study, we considered that the norm restricted interval only depends on a fuzzy interval of the clustering results. So the range of the interval needs to be further optimized. Although the fuzzy neural network has strong coupling between the fitting effect and the expression input, more input will cause a significantly large fuzzy rule table. Thus, scholars should focus on reducing the computational complexity.

## ■ AUTHOR INFORMATION

### Corresponding Author

Li Yang – College of Electrical Information Engineering, Northeast Petroleum University, Daqing 163318, China; [orcid.org/0000-0002-8089-1557](https://orcid.org/0000-0002-8089-1557); Email: 19696163@qq.com

### Authors

Tianyi Liu – College of Electrical Information Engineering, Northeast Petroleum University, Daqing 163318, China  
 Weijian Ren – College of Electrical Information Engineering, Northeast Petroleum University, Daqing 163318, China  
 Wenfeng Sun – College of Electrical Information Engineering, Northeast Petroleum University, Daqing 163318, China

Complete contact information is available at: <https://pubs.acs.org/10.1021/acsomega.1c02107>

### Notes

The authors declare no competing financial interest.

## ■ ACKNOWLEDGMENTS

This work was supported by the National Natural Science Foundation of China to research on the mechanism of rock breaking by electric pulse plasma based on the thermal-mechanical coupling effect (No. 51974090) and the Guiding Innovation Fund of Northeast Petroleum University to research on the response mechanism and the fracture mechanism of rock under electric pulse excitation (No. 2018ydl-06).

## ■ REFERENCES

- (1) Lin, S. X. Drilling Parameters Optimization Technology Status and Development Trend. *China Pet. Mach.* **2016**, *44*, 29–33.

- (2) Salaheldin, E. Real-Time Prediction of Rate of Penetration in S-Shape Well Profile Using Artificial Intelligence Models. *Sensors* **2020**, *20*, No. 3506.
- (3) Zhou, Y.; Chen, X.; Wu, M.; Cao, W. Modeling and coordinated optimization method featuring coupling relationship among sub-systems for improving safety and efficiency of drilling process. *Appl. Soft Comput.* **2020**, *99*, No. 106899.
- (4) Hegde, C.; Daigle, H.; Millwater, H.; Gray, K. Analysis of rate of penetration (rop) prediction in drilling using physics-based and data-driven models. *J. Pet. Sci. Eng.* **2017**, *159*, 295–306.
- (5) Ahmed, O. S.; Adeniran, A. A.; Ariffin, S. Computational intelligence based prediction of drilling rate of penetration: a comparative study. *J. Pet. Sci. Eng.* **2019**, *172*, 1–12.
- (6) Zhou, Y.; Chen, X.; Zhao, H.; Wu, M.; Liu, H. A novel rate of penetration prediction model with identified condition for the complex geological drilling process. *J. Process Control* **2021**, *100*, 30–40.
- (7) Su, X.; Sun, J.; Gao, X.; Wang, M. Prediction method of drilling rate of penetration based on GBDT algorithm. *Comput. Appl. Software* **2019**, *36*, 87–92.
- (8) Eskandarian, S.; Bahrami, P.; Kazemi, P. A comprehensive data mining approach to estimate the rate of penetration: application of neural network, rule based models and feature ranking. *J. Pet. Sci. Eng.* **2017**, *156*, 605–615.
- (9) Wang, W.; Liu, X.; Dou, P.; Lin, H.; Tao, L. A ROP prediction method based on neural network for the deep layers. *Oil Drill. Prod. Technol.* **2018**, *40*, 121–124.
- (10) Zhao, Y.; Noorbakhsh, A.; Koopialipoor, M.; Azizi, A.; Tahir, M. M. A new methodology for optimization and prediction of rate of penetration during drilling operations. *Eng. Comput.* **2019**, *36*, 587–595.
- (11) Kahraman, S. Estimating the penetration rate in diamond drilling in laboratory works using the regression and artificial neural network analysis. *Neural Process. Lett.* **2016**, *43*, 523–535.
- (12) Liu, S. W.; Sun, J. M.; Gao, X.; Wang, M. Analysis and Establishment of Drilling Speed Prediction Model for Drilling Machinery Based on Artificial Neural Networks. *Comput. Sci.* **2019**, *46*, 605–608.
- (13) Hadi, F.; Habibollah, B. Applying Improved Artificial Neural Network Model to Evaluate Drilling Rate Index. In *Tunnelling and Underground Space Technology*; Elsevier, 2017.
- (14) Brenjkar, E.; Delijani, E. B.; Karroubi, K. Prediction of penetration rate in drilling operations: a comparative study of three neural network forecast methods. *J. Pet. Explor. Prod.* **2021**, *11*, 805–818.
- (15) Shi, X.; Liu, G.; Gong, X.; Zhang, J.; Wang, J.; Zhang, H. An efficient approach for real-time prediction of rate of penetration in offshore drilling. *Math. Probl. Eng.* **2016**, *2016*, No. 3575380.
- (16) Ashrafi, S. B.; Anemangely, M.; Sabah, M.; Ameri, M. J. Application of hybrid artificial neural networks for predicting rate of penetration (ROP): A case study from Marun oil field. *J. Pet. Sci. Eng.* **2019**, *175*, 604–623.
- (17) Sabah, M.; Talebkeikhah, M.; Wood, D. A.; Khosravianian, R.; Anemangely, M.; Younesi, A. A machine learning approach to predict drilling rate using petrophysical and mud logging data. *Earth Sci. Inf.* **2019**, *12*, 319–339.
- (18) Liao, X.; Khandelwal, M.; Yang, H.; Koopialipoor, M.; Murlidhar, B. R. Effects of a proper feature selection on prediction and optimization of drilling rate using intelligent techniques. *Eng. Comput.* **2019**, *36*, 499–510.
- (19) Anemangely, M.; Ramezanzadeh, A.; Tokhmechi, B.; Molaghab, A.; Mohammadian, A. Drilling rate prediction from petrophysical logs and mud logging data using an optimized multilayer perceptron neural network. *J. Geophys. Eng.* **2018**, *15*, 1146–1159.
- (20) Anand, G.; Alagumurthi, N.; Elansezhian, R.; Elansezhian, K.; Palanikumar, N.; Venkateshwaran. Investigation of drilling parameters on hybrid polymer composites using grey relational analysis, regression, fuzzy logic, and ann models. *J. Braz. Soc. Mech. Sci. Eng.* **2018**, *40*, No. 214.
- (21) Hassan, A.; Elkatatny, S.; Al-Majed, A. Coupling rate of penetration and mechanical specific energy to Improve the efficiency of drilling gas wells. *J. Nat. Gas Sci. Eng.* **2020**, *83*, No. 103558.
- (22) Fang, Y.; Fei, J.; Wang, T. Adaptive Backstepping Fuzzy Neural Controller Based on Fuzzy Sliding Mode of Active Power Filter. *IEEE Access* **2020**, 96027–96035.
- (23) He, W.; Dong, Y. T. Adaptive Fuzzy Neural Network Control for a Constrained Robot Using Impedance Learning. *IEEE Trans. Neural Networks. Learn. Syst.* **2018**, *99*, 1174–1186.
- (24) Tang, Y.; Zhao, Y. P.; Jiang, J. S.; Xiao, P. B. Application of Fuzzy Neural Network Control Strategy in Automobile Stability Control. *Mach. Des. Manuf.* **2020**, *3*, 81–84.
- (25) Zhong, Y. H.; Miao, D. H.; Zhao, M. H.; Shao, D. G.; Zhu, S. H. Water quality evaluation method based on T-S fuzzy neural network and its application in Sishui watershed. *Hydro Sci. Cold Zone Eng.* **2020**, *3*, 20–24.
- (26) Cai, J.; Luo, J.; Wang, S.; Yang, S. Feature selection in machine learning: A new perspective. *Neurocomputing* **2018**, *300*, 70–79.
- (27) Abualigah, L. M.; Khader, A. T.; Hanandeh, E. S. A new feature selection method to improve the document clustering using particle swarm optimization algorithm. *J. Comput. Sci.* **2018**, *25*, 456–466.
- (28) Majdi, M.; Seyedali, M. Hybrid Whale Optimization Algorithm with simulated annealing for feature selection. *Neurocomputing* **2017**, *260*, 302–312.
- (29) Li, Q.; Qiao, F.; Mao, A.; Mccreight, C. Characterizing the Importance of Criminal Factors Affecting Bus Ridership using Random Forest Ensemble Algorithm. *Transp. Res. Rec.* **2019**, *2673*, 864–876.
- (30) Zhang, L. Z.; Nawaf, R. A.; Luo, G.; Yao, Z.; Li, Y. A Hybrid Forecasting Framework Based on Support Vector Regression with a Modified Genetic Algorithm and a Random Forest for Traffic Flow Prediction. *Tsinghua Sci. Technol.* **2018**, *23*, 479–492.
- (31) Nabipour, N.; Mosavi, A.; Hajnal, E.; Nadai, L.; Chau, K. W. Modeling climate change impact on wind power resources using adaptive neuro-fuzzy inference system. *Eng. Appl. Comput. Fluid Mech.* **2020**, *14*, 491–506.
- (32) Baghban, A.; Jalali, A.; Shafiee, M.; Ahmadi, M. H.; Chau, K. W. “Developing an ANFIS based Swarm Concept Model for Estimating Relative Viscosity of Nanofluids”. *Eng. Appl. Comput. Fluid Mech.* **2019**, *13*, 26–39.
- (33) Li, G. Y.; Liu, P. An Generalized Predictive Control Using Recurrent Fuzzy Neural Network. *J. Taiyuan Univ. Technol.* **2012**, *43*, 11–15.
- (34) Zhang, S.; Guo, X. Research on K-means Algorithm Based on Fuzzy Clustering. *J. Jilin Eng. Norm. Univ.* **2019**, *35*, 86–88.
- (35) Zhao, Z.; Bai, B.; Shiming, H. E.; Liu, B. Optimization of Fast Drilling Technology for Ultra-Deep Wells in the Shunbei Oilfield. *Pet. Drill. Tech.* **2017**, *45*, 8–13.
- (36) Shi, Y. Completed drilling depth of Shunbei 5–5h well in Northwest Oilfield: 8520 m. *Pet. Drill. Prod. Technol.* **2018**, *40*, 23.